Biochemistry

Article

Cite This: Biochemistry 2018, 57, 6780−6786

pubs.acs.org/biochemistry

Internalization of Methotrexate Conjugates by Folate Receptor-α

Eugénia Nogueira,[†,∥] Marisa P. Sárria,[†,‡,∥,⊥] Nuno G. Azoia,[†,∥,#] Egipto Antunes,[†] Ana Loureiro,[†] Diana Guimarães,[†] Jennifer Noro,[†] Alexandra Rollett,[§] Georg Guebitz,[§] and Artur Cavaco-Paulo*[,†]

[†]Centre of Biological Engineering, University of Minho, Campus of Gualtar, 4710-057 Braga, Portugal

[‡]Centre of Molecular and Environmental Biology (CBMA), Department of Biology, University of Minho, Campus of Gualtar, 4710-057 Braga, Portugal

[§]Institute for Environmental Biotechnology, University of Natural Resources and Life Sciences, Vienna, A-3430 Tulln, Austria

ABSTRACT: The folate antagonist methotrexate is a cytotoxic drug used in the treatment of several cancer types. The entry of methotrexate into the cell is mediated by two main transport systems: the reduced folate carrier and membrane-associated folate receptors. These transporters differ considerably in their mechanism of (anti)folate uptake, substrate specificity, and tissue specificity. Although the mechanism of action of the reduced folate carrier is fairly well-established, that of the folate receptor has remained unknown. The development of specific folate receptor-targeted antifolates would be accelerated if additional mechanistic data were to become available. In this work, we used two fluorescently labeled conjugates of methotrexate, differently linked at the terminal groups, to clarify the uptake mechanism by folate receptor-α. The results demonstrate the importance of methotrexate amino groups in the interaction with folate receptor-α.

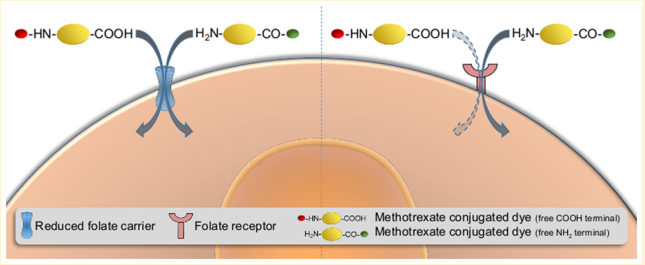

The folate antagonist methotrexate (MTX) was introduced into oncology as a cytotoxic antiproliferative agent that has been used in the treatment of various cancer types for decades.[1] It is an antimetabolite that inhibits dihydrofolate reductase (DHFR), which is an enzyme involved in the biosynthetic pathway of nucleotides, and MTX is therefore highly toxic to rapidly dividing cancer cells.[2]

The first pivotal step in the cellular pharmacology of MTX is its entry into the cell, which can be mediated by two general transport systems: the reduced folate carrier (RFC) and membrane-associated folate receptors (FRs). These transport routes are physiologically and pharmacologically relevant for immunocompetent cells because they facilitate the uptake of natural reduced folate cofactors and folate antagonists, such as MTX.[3] The RFC and FRs differ considerably in their mechanism of (anti)folate uptake (transmembrane carrier vs endocytosis), substrate specificity (low-affinity folic acid/high-affinity MTX vs high-affinity folic acid/low-affinity MTX), and tissue specificity (constitutive vs restricted expression) (Figure 1).

The membrane-spanning anion transporter RFC has a constitutive expression in essentially all human tissues, providing a high-affinity bidirectional exchange mechanism for reduced folate cofactors and MTX (K_m = 1−10 μM). Inversely, the RFC binding affinity for folic acid is low (K_i = 200−400 μM).[4,5]

A second folate transport mechanism is mediated by FR, a particulate form of folate binding proteins, which are anchored to the cell membrane by glycosylphosphatidylinositol (GPI) residues. FRs have a mass of 38−40 kDa and are encoded by two genes (FR α and β) with differential tissue expression. The α-isoform of FR is overexpressed in specific types of cancer (e.g., ovarian cancer),[6] while the β isoform on activated macrophages.[7] The third member of this gene family, γ-type, is a secretory protein, from hematopoietic cells, because of the lack of a signal for GPI attachment.[8] Unlike RFC, FR exhibits a much greater affinity for folic acid and 5-methyltetrahydrofolate (K_d = 1−10 nM) but lower for other reduced folates and MTX (K_d = 10−300 nM). FRs also have different properties in terms of energy, ion, and pH dependence.[4] The level of binding of folate to FR is decreased after energy depletion and in the absence of chloride anion but does not decrease until the pH falls below 5.0.[9]

The functional activity of the RFC-mediated cellular traffic of antifolates with antitumor activity *in vivo* is fairly well-established.[5] On the contrary, the exact role and mechanism of action of the FRα have remained unclear.[10] In 2013, the structure−activity relationship for molecular (high-affinity) recognition of folate and folate conjugates by FRα was disclosed.[11] It was demonstrated that FRα has a globular structure stabilized by eight disulfide bonds and contains a folate binding pocket formed of conserved residues (across all receptor subtypes).[11] The molecular model reveals that the glutamate moiety is solvent-exposed and projects from the receptor's pocket entrance, enabling cargo attachment without obstructing FRα binding.[11] This structure helps explain the low binding affinity of MTX for FRα, because it shows that there is a steric impediment of a specific amino group that interferes with the binding to the receptor.

Received: May 30, 2018
Revised: November 15, 2018
Published: November 19, 2018

DOI: 10.1021/acs.biochem.8b00607
Biochemistry 2018, 57, 6780−6786

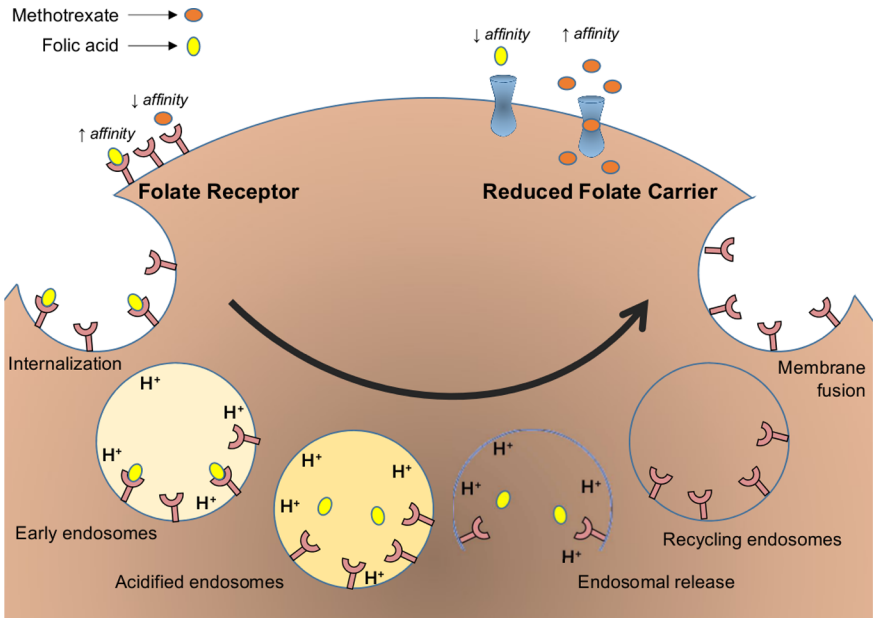

Figure 1. Schematic representation of folate receptor-mediated endocytosis and methotrexate influx. The folic acid has a 100−200-fold greater affinity for the folate receptor than for the reduced folate carrier. Inversely, the reduced folate carrier binding affinity for methotrexate is higher.

Knowing the molecular recognition details and considering that MTX is transported into cells via the FR rather than through facilitative transporters (expressed in normal tissues), one could not expect damage to normal cells.[12] Therefore, FRα-targeted therapy should focus on overcoming the affinity and specificity for MTX, over RFC. This could be achieved through engineering of molecules that take advantage of the many solvent-filled cavities that surround ligands in the folate receptor binding cleft.[12]

In the study presented here, we elucidate the mechanism of uptake of MTX by FRα. Two fluorescently labeled conjugates of MTX, differently linked at the terminal groups, were used for cellular uptake, and molecular docking and molecular dynamics simulations were performed to validate their findings.

METHODS

Fluorescent Labeling of MTX. MTX was labeled with the amino-reactive fluorescent dye Red Mega 520 NHS-ester (fluorescent red), as previously described for folic acid.[13] Briefly, 140 μL of an MTX solution [3.7 mg/mL in a 3:1 mixture of 50 mM bicarbonate buffer (pH 9) and dimethylformamide (DMF)] was mixed with 28 μL of a fluorescent red solution (20 mg/mL in DMF), and 200 μL of DMF was added. The mixture was shaken for 4 h at 25 °C under light protection. The product was purified by size exclusion chromatography using a HiTrap Desalting column (GE Healthcare Europe GmbH, Vienna, Austria) installed on an Äkta Purifier system (Amersham Pharmacia Biotech, Uppsala, Sweden) with 50 mM potassium phosphate and 100 mM NaCl (pH 7) as the eluent, at the flow rate of 1 mL/min, to remove excess fluorescent red. Fractions, which showed absorbance at 520 nm for fluorescent red and 368 nm for MTX, were collected. Electrospray ionization (ESI) was performed in a Thermo Finnigan LxQ mass detector (Linear Ion Trap). The mass detector was susceptible of analysis in full scan mode, SIM and MS/MS with negative ionization. The mass spectral range was from 50 to 2000. The capillary voltage was 29 V. MTX concentrations were determined photometrically by comparison with a calibration curve. According to the manufacturer's instructions (Sigma-Aldrich Co., St. Louis, MO), fluorescent Mega dyes have a large Stokes shift among excitation and emission maxima, compatible with the same excitation conditions (light source or filter arrangement) as the fluorescent green fluorescein isothiocyanate (FITC). As such, the commercial fluorescent green conjugate of MTX (Molecular ProbeslLife Technologies), linked through the carboxyl groups, was further considered for the cellular uptake experiments.

Cell Culture Conditions. The epithelial cancer cell line KB (ATCCCCL-17) and the MDA-MB-435S human melanoma cells (ATCCHTB-129) were obtained from the American Type Culture Collection. The KB cell line was maintained in Roswell Park Memorial Institute (RPMI)-1640 Medium (without folic acid) containing 2 mM L-glutamine and 2 mg/mL sodium bicarbonate supplemented with 10% (v/v) fetal bovine serum (FBS) and a 1% (v/v) penicillin/streptomycin solution. The MDA-MB-435S cell line was maintained in Dulbecco's modified Eagle's medium (DMEM) containing 4 mM L-glutamine, 4.5 g/L glucose, and 1.5 g/L sodium bicarbonate supplemented with 10% (v/v) FBS and a 1% (v/v) penicillin/streptomycin solution. Cells were maintained at 37 °C in a humidified atmosphere of 5% CO_2. Cells were routinely subcultured over 2 to 3 days.

FR Confirmation by Real-Time Quantitative Polymerase Chain Reaction (qPCR). Cell lysates of different-origin cancer lines were collected, and total RNA was extracted using the "SV Total RNA Isolation System", according to the manufacturer's protocol (Promega Corp.). Following column elution with 30 μL of RNase-free water, the RNA concentration was determined by measuring the absorbance at 260 nm in a NanoDrop ND-1000 spectrophotometer (A_{260} = 1−40 μg/mL) (Nanodrop Technologies). The A_{260}/A_{280} ratio was calculated to estimate RNA purity. Reverse transcription was performed using the "iScriptTM cDNA synthesis kit" (Bio-Rad Laboratories). Unique blended oligo(dT) and random hexamer primers were incubated according to the manufacturer's protocol as follows: 5 min at 25 °C, 60 min at 42 °C, 5 min at 85 °C, and hold

DOI: 10.1021/acs.biochem.8b00607
Biochemistry 2018, 57, 6780−6786

at 4 °C. For confirmation of FRα and RFC expression levels, TaqMan probe-based gene expression assays (Applied Biosystems, Spain) were considered: Hs01124177_m1 and Hs00953345_m1, respectively. Real-time qPCRs were performed in a CFX96 Real-Time PCR Detection System, with a C1000TM thermal cycler (Bio-Rad Laboratories). The amplification process used the following conditions: UNG incubation at 50 °C for 2 min, polymerase activation at 95 °C for 10 min, denaturation at 95 °C for 15 s, and annealing/extension at 60 °C for 60 s, for 50 cycles (data collection). A stable endogenous control gene, cyclin-dependent kinase inhibitor 1A, CDKN1A (TaqMan assay Hs00355782_m1; Applied Biosystems, Spain), was used for normalization of the expression values.

Uptake Experiments. The FRα-positive cells (KB cancer cell line) and MDA-MB-435S cells (negative control) were harvested from the culture vessel during their S-phase (i.e., until a monolayer, with a confluence of >60%, was obtained) and seeded at a density of 100000 cells/mL (24-well microplates) for the uptake experiments. After an overnight period to ensure optimal adhesion, the culture medium was removed, and adherent cells were washed twice with acidic phosphate-buffered saline (pH 3.5) to remove bound folic acid. The MTX conjugates were diluted in Hanks' balanced salt solution (folate-free) at a nontoxic (data not shown) concentration of 6 μM (adjusted for antifolate concentration) and incubated in cancer cells for 4 h. The same experiment was repeated using medium containing 113 μM free folic acid (Sigma) and calcium folinate (TCI) to determine the effect of FR and RFC blockade, respectively. The cultures were maintained under a humidified atmosphere containing 5% CO_2 in a 37 °C incubator. The internalized concentration of MTX conjugates was determined, considering the fluorescence intensity measured (PerkinElmer LS-50B luminescence spectrometer) upon lysis of the exposed cells. All values were corrected by the intensity/molarity ratio, according to calibration curves of fluorescently labeled conjugates.

Molecular Docking Simulations. The computational models of FRα, RFC, and MTX have different origins. The FRα model corresponds to entry 4KM6 of the RCSB Protein Data Bank (PDB),[14] that is an X-ray diffraction of human FRα (FOLR1) at acidic pH. The software Modeler (https://salilab.org/modeller)[15] was used to obtain a three-dimensional model of RFC protein, through homology with a structure of a transmembrane glucose transporter obtained by X-ray diffraction (PDB entry 4ZW9),[16] due to the lack of a full crystallographic model of RFC. Finally, the MTX structure was obtained using the "Automated Topology Builder (ATB) and Repository" online server (https://atb.uq.edu.au/)[17] using AM1-optimized geometry and MOPAC charges.

The models of FRα, RFC, and MTX were preprocessed with Autodock tools[18] to correct the charges, the hydrogens, and the bond flexibility when needed. Later, Autodock Vina[19] was used to perform the docking simulations between FRα and MTX and between RFC and MTX to evaluate the binding affinity between them. All docking calculations were performed with one 5 nm × 5 nm × 5 nm box centered on the FR active site, and the exhaustiveness was varied between 80 and 800.

Molecular Dynamics Simulations. The simulations were performed with the GROMACS 4.6.5[20] package using the GROMOS 54A7 force field.[21,22] The initial configurations of the protein−MTX conjugates were the result of docking simulations with higher binding energies. These structures were solvated and simulated for a few nanoseconds (~10 ns). The bond lengths of the proteins were constrained with LINCS,[23] and those for water with SETTLE.[24] Nonbonded interactions were calculated using a twin-range method, with short- and long-range cutoffs of 0.8 and 1.4 nm, respectively. Neighbor searching was performed up to 1.4 nm and updated every two steps. A time step of integration of 2 fs was used. A reaction field correction for the electrostatic interactions was applied using a dielectric constant of 54.[25] The single-point charge model[26] was used for water molecules. The initial systems were energy minimized for 2000 steps using the steepest descent method, with all heavy atoms harmonically restrained using a force constant of 10^3 kJ mol^{-1} nm^{-2}.

The systems were initialized in the canonical ensemble (*NVT*) for 50 ps, with all heavy atoms harmonically restrained using a force constant of 10^3 kJ mol^{-1} nm^{-2}. The simulation was then continued for picoseconds in the isothermal−isobaric ensemble (*NPT*), with the heavy atoms harmonically restrained with the same force constant. Finally, to allow the equilibration of the system properties, the simulations were further extended in the *NPT* ensemble with position restraints applied to only the α-carbons. Pressure control was implemented using the Berendsen barostat,[27] with a reference pressure of 1 bar, a relaxation time of 0.5 ps, and an isothermal compressibility of 4.5 × 10^{-5} bar^{-1}. Temperature control was set using the V-rescale[27,28] thermostat at 300 K with coupling constants of 0.025 ps in the first two initialization steps and 0.1 ps for the rest of the simulations. At least three replica systems were simulated for each condition, from 50 ns using different initial velocities taken from a Maxwell−Boltzman distribution at 300 K. GROMACS tools were used to evaluate several properties of the systems, such as the pressure, temperature, and surface accessible solvent area, providing insights into the correct modeling of the protein−MTX interaction.

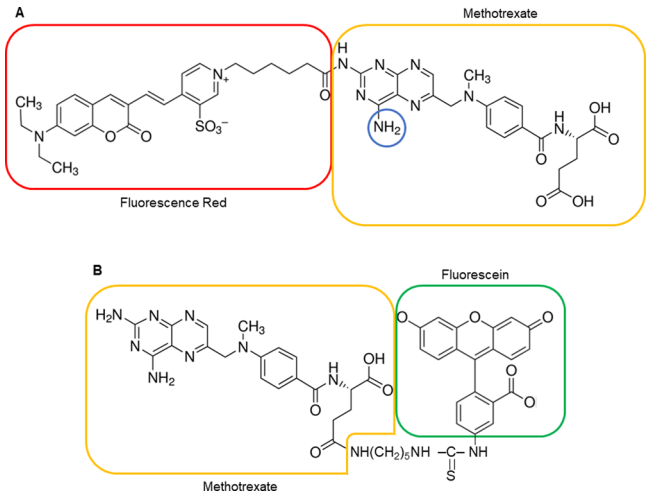

Figure 2. Molecular structures (most probable) of the tested conjugates. (A) Red Mega-HN-MTX-COOH and (B) H_2N-MTX-CO-FITC. Fluorescent red dye can also be linked to the amino group marked with a circle, but because the conjugate was purified by size exclusion chromatography, the occurrence of a 2/1 (Mega dye/MTX) conjugate is excluded, as it would have a larger size and therefore a shorter retention time. The MTX−Red Mega 520 conjugate was analyzed by ESI, and the observed mass peak (m/z 951.02) corresponds to the theoretical molecular weight (data not shown). The fluorescent green dye is linked to the carboxyl groups of MTX as presented, according to the manufacturer's information (Molecular Probes|Life Technologies).

DOI: 10.1021/acs.biochem.8b00607
Biochemistry 2018, 57, 6780−6786

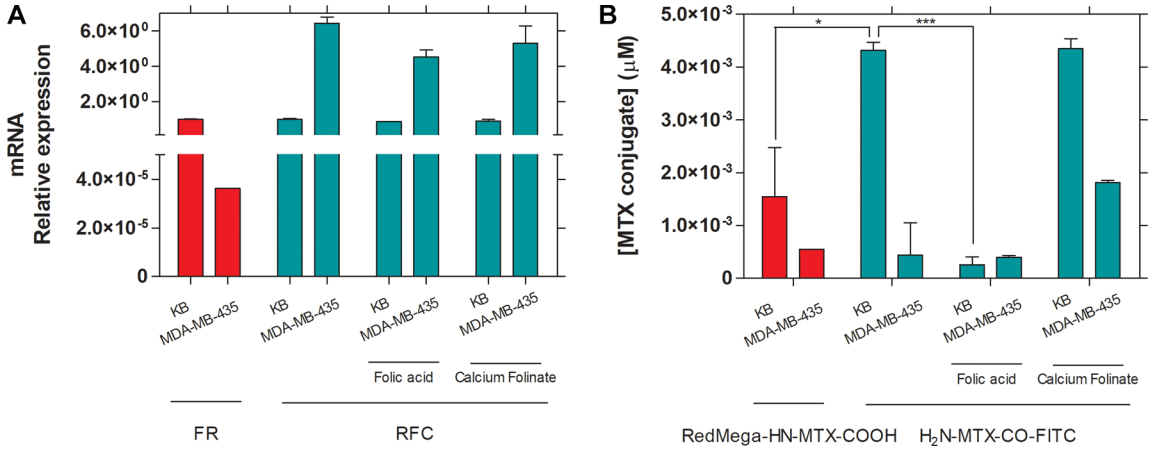

Figure 3. (A) Analysis of FRα and RFC expression levels in human cancer cell lines. (B) Uptake concentrations of the fluorescently labeled MTX conjugates by cancer cell lines: FRα-positive KB and FRα-negative MDA-MB-435S. RFC expression levels and uptake of the H_2N-MTX-CO-FITC conjugate were also analyzed after incubation of cells with folic acid and calcium folinate. Values are presented as means ± the standard error of two independent experiments. Differences were tested for statistical significance by a one-way analysis of variance (*P < 0.005; ***P < 0.001).

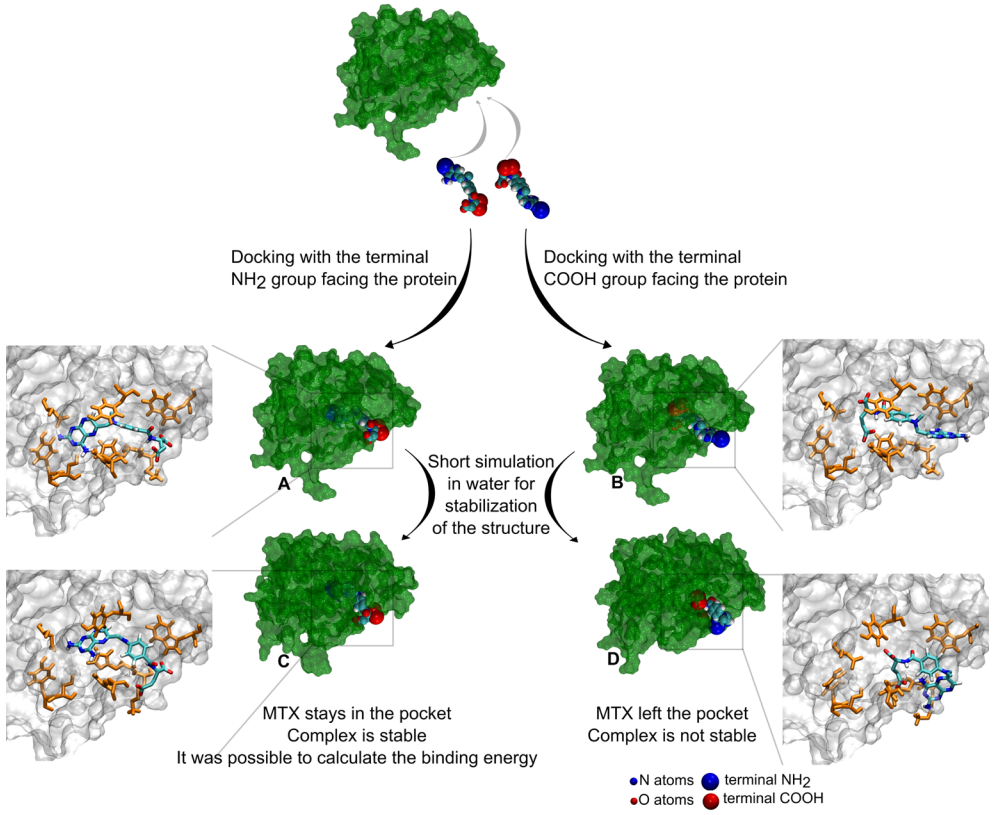

Figure 4. Molecular docking and molecular dynamics simulations. (A) Docking result showing MTX at the active site of FRα with the amino groups facing the protein. The docking result was the starting point of the molecular dynamics. (B) Docking result showing MTX at the active site of FRα with the carbonyl groups facing the protein. The docking result was the starting point of the molecular dynamics. (C) System A after a simulation run of 1 ns to ensure stabilization. This was the starting point of the umbrella pulling procedure. (D) System B after a simulation run of 1 ns to ensure stabilization. The configuration derived from the docking was not stable, and after a short simulation, MTX is no longer at the active site of the receptor.

In addition, pulling simulations were performed with FR−MTX and RFC−MTX conjugates, with a constant force of 1000 kJ mol^{-1} nm^{-2} and a rate of 0.1 nm/ns applied to the MTX molecule. The force applied in the MTX molecule obliges the molecule to exit from the active sites of the tested proteins. The MTX had its carboxyl group termination facing the solvent in both cases. Later an umbrella sampling methodology[29] was applied to calculate the potential of mean force for the process of MTX molecules exiting the FRα and RFC proteins.

RESULTS AND DISCUSSION

In this work, two fluorescently labeled conjugates of MTX, differently linked at the terminal groups (Figure 2), were considered for cellular uptake. Because high levels of FRα were

DOI: 10.1021/acs.biochem.8b00607
Biochemistry 2018, 57, 6780−6786

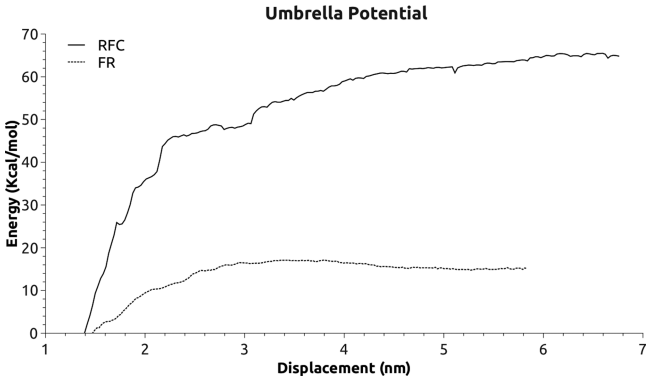

Figure 5. Potentials of mean force of MTX with RFC and FRα.

reported in a wider spectrum of epithelial-origin tissues,[30] human epithelial adenocarcinoma cells of the mammary gland were selected for exposure to the antifolate conjugates, in comparison to a negative control. The FRα expression levels of the different-origin cancer cells were quantified using a standardized real-time qPCR detection system. The concentration of the conjugates internalized (adjusted for MTX concentration) was determined, considering the fluorescence measured in the lysates of the exposed cells. To ascertain the "targetability" of FRα, molecular docking simulations of the FRα−MTX complex were performed.

This study adds information to the current understanding of the structural underpinnings of the transport of antifolate-based derivatives. Moreover, the interference of the chemical nature of their free terminal groups on the affinity and/or specificity of the molecular interactions involved in their cellular uptake was evaluated. The functional chemical groups of the MTX conjugates implicated in the binding to the surface-associated receptor, and their potential as a "tool" to surmount the membrane-spanning anion transporter, avoiding significant side effects and dose-limiting toxicities, are discussed.

Prior to cellular uptake experiments, FRα expression levels of the different-origin human cancer cells were confirmed. Real-time qPCR data analysis revealed higher expression levels of FRα in the KB cancer cell line and negligible levels in the MDA-MB-435S cell line (Figure 3A).[11] Although posttranscriptional regulation can occur, previous studies showed that the level of protein expression of FR[31,32] and RFC[33,34] in several cancer cell lines is directly proportional to mRNA levels.

The uptake concentration of the MTX conjugates, differently linked at the terminal functional groups, showed significant interaction among the selected factors. For FRα-positive cells, KB, significant statistical differences were observed among the internalized concentrations of the two MTX conjugates, whereas for the FRα-negative cells, MDA-MB-435S, negligible differences were observed (Figure 3B). Comparable amounts of both MTX conjugates, with either terminus blocked, were taken up similarly by FRα-negative cells. It is noteworthy that, although H_2N-MTX-CO-FITC internalization remains unaltered after incubation with a high-affinity FR substrate (folic acid),[35] as expected, it is possible to observe an increase in the level of internalization after incubation with the high-affinity RFC substrate (calcium folinate).[36] Once RFC expression remains similar after incubation with the high-affinity RFC substrate (Figure 3A), one can speculate that another uptake mechanism is present or is activated in the presence of a huge quantity of the calcium folinate.

Higher concentrations of the H_2N-MTX-CO-FITC conjugate were taken up by FRα-positive cells compared to that of the Red Mega-HN-MTX-COOH conjugate (Figure 3B). This result provides a proof of concept of higher passage of MTX via FRα when the amino groups are free. Furthermore, as expected, the level of internalization of the H_2N-MTX-CO-FITC conjugate decreases after incubation with the high-affinity FR substrate, folic acid, remaining unaltered after incubation with the high-affinity RFC substrate, calcium folinate.

The receptors FRα and FRβ have high degrees of sequence identity (82%) and similarity (92%), with their binding sites being highly conserved, with only two divergent residues (V129α/F123β and K158α/R152β).[12] Although we did not perform studies with cell lines expressing FRβ, a behavior similar to that of FRα would be expected.

The ability of the conjugate with free amino groups to bind to FRα was further confirmed by molecular docking and molecular dynamics simulations, as shown in Figure 4. Molecular docking experiments initially suggested that MTX is capable of binding to FRα using either the terminal amino group (Figure 4A) or the terminal carboxylic group (Figure 4B). However, stabilization of these docking structures in water, using molecular dynamics simulation tools, showed that the complex is stable only if the amino groups are facing the FRα pocket and not the opposite.

Taking into account the molecular dynamics simulations, we calculated the binding energy between the two transport systems and MTX, using an umbrella sampling technique to calculate the potential of mean force. The final result demonstrates that the complex of MTX and RFC is stronger, with a binding energy of approximately 65 kcal mol^{-1}, comparatively

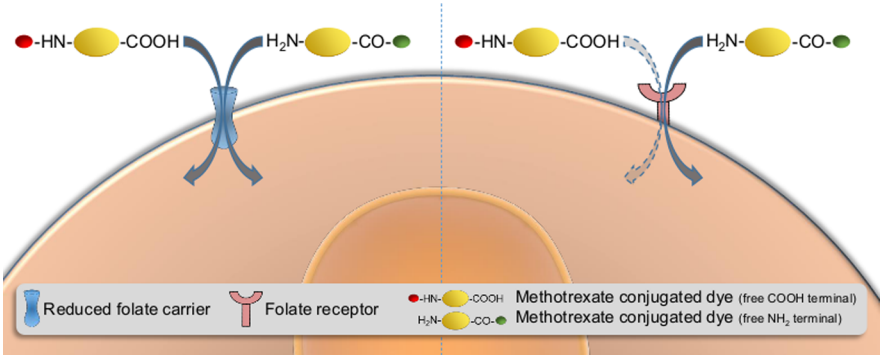

Figure 6. Schematic representation of the proposed mechanism showing internalization mechanisms of MTX conjugates, in FRα-negative and -positive cells.

DOI: 10.1021/acs.biochem.8b00607
Biochemistry 2018, 57, 6780−6786

with FRα, with a binding energy of approximately 15 kcal mol^{-1} (Figure 5).

In summary, the obtained outcomes provide a rationale for designing more specific drugs for selective approaches. Modulation of the MTX terminal groups might be a potentially useful strategy for improved mediated transport targeting through the FRα system on cancer cells (Figure 6). A major outcome anticipated from this study is the development of the next generation of FR-targeted therapeutics.

AUTHOR INFORMATION

Corresponding Author

*E-mail: artur@deb.uminho.pt.

ORCID

Artur Cavaco-Paulo: 0000-0001-7204-2064

Present Addresses

[⊥]M.P.S.: International Iberian Nanotechnology Laboratory, 4715-330 Braga, Portugal.

[#]N.G.A.: Centre for Nanotechnology and Smart Materials (CeNTI), 4760-034 Vila Nova de Famalicão, Portugal.

Author Contributions

[‖]E.N., M.P.S., and N.G.A. contributed equally to this work.

Funding

E.A. (SFRH/BD/122952/2016) and J.N. (SFRH/BD/121673/2016) hold scholarships from the Portuguese Foundation for Science and Technology (FCT). This study was supported by the FCT under the scope of the strategic funding of the UID/BIO/04469/2013 unit and the COMPETE 2020 (POCI-01-0145-FEDER-006684) and BioTecNorte operation (NORTE-01-0145-FEDER-000004) funded by the European Regional Development Fund under the scope of Norte2020—Programa Operacional Regional do Norte. This work has also received funding from the European Union 7th Framework Programme (FP7/2007−2013), under Grant Agreement NMP4-LA-2009-228827 NANOFOL, and the Horizon 2020 research and innovation program under Grant Agreement NMP-06-2015-683356 FOLSMART.

Notes

The authors declare no competing financial interest.

REFERENCES

(1) anonymous (1965) New treatment schedule with improved survival in childhood leukemia: Intermittent parenteral vs daily oral administration of methotrexate for maintenance of induced remission. *JAMA 194* (1), 75−81.

(2) Lennard, L. (1999) Therapeutic drug monitoring of anti-metabolic cytotoxic drugs. *Br. J. Clin. Pharmacol. 47* (2), 131−143.

(3) Van Der Heijden, J. W., Oerlemans, R., Dijkmans, B. A. C., Qi, H., Laken, C. J. V. D., Lems, W. F., Jackman, A. L., Kraan, M. C., Tak, P. P., Ratnam, M., and Jansen, G. (2009) Folate receptor β as a potential delivery route for novel folate antagonists to macrophages in the synovial tissue of rheumatoid arthritis patients. *Arthritis Rheum. 60* (1), 12−21.

(4) Brzezinska, A., Winska, P., and Balinska, M. (2000) Cellular aspects of folate and antifolate membrane transport. *Acta Biochim. Pol. 47* (3), 735−49.

(5) Matherly, L. H., and Goldman, D. I. (2003) Membrane transport of folates. *Vitam. Horm. 66*, 403−56.

(6) Salazar, M. D., and Ratnam, M. (2007) The folate receptor: what does it promise in tissue-targeted therapeutics? *Cancer Metastasis Rev. 26* (1), 141−52.

(7) Shen, J., Chelvam, V., Cresswell, G., and Low, P. S. (2013) Use of Folate-Conjugated Imaging Agents To Target Alternatively Activated Macrophages in a Murine Model of Asthma. *Mol. Pharmaceutics 10* (5), 1918−1927.

(8) Shen, F., Ross, J. F., Wang, X., and Ratnam, M. (1994) Identification of a novel folate receptor, a truncated receptor, and receptor type beta in hematopoietic cells: cDNA cloning, expression, immunoreactivity, and tissue specificity. *Biochemistry 33* (5), 1209−15.

(9) Spinella, M. J., Brigle, K. E., Sierra, E. E., and Goldman, I. D. (1995) Distinguishing between folate receptor-alpha-mediated transport and reduced folate carrier-mediated transport in L1210 leukemia cells. *J. Biol. Chem. 270* (14), 7842−9.

(10) Assaraf, Y. (2007) Molecular basis of antifolate resistance. *Cancer Metastasis Rev. 26* (1), 153−181.

(11) Chen, C., Ke, J., Zhou, X. E., Yi, W., Brunzelle, J. S., Li, J., Yong, E.-L., Xu, H. E., and Melcher, K. (2013) Structural basis for molecular recognition of folic acid by folate receptors. *Nature 500* (7463), 486−489.

(12) Wibowo, A. S., Singh, M., Reeder, K. M., Carter, J. J., Kovach, A. R., Meng, W., Ratnam, M., Zhang, F., and Dann, C. E. (2013) Structures of human folate receptors reveal biological trafficking states and diversity in folate and antifolate recognition. *Proc. Natl. Acad. Sci. U. S. A. 110* (38), 15180−15188.

(13) Rollett, A., Reiter, T., Nogueira, P., Cardinale, M., Loureiro, A., Gomes, A., Cavaco-Paulo, A., Moreira, A., Carmo, A. M., and Guebitz, G. M. (2012) Folic acid-functionalized human serum albumin nanocapsules for targeted drug delivery to chronically activated macrophages. *Int. J. Pharm. 427* (2), 460−466.

(14) Wibowo, A. S., Singh, M., Reeder, K. M., Carter, J. J., Kovach, A. R., Meng, W., Ratnam, M., Zhang, F., and Dann, C. E., 3rd (2013) Structures of human folate receptors reveal biological trafficking states and diversity in folate and antifolate recognition. *Proc. Natl. Acad. Sci. U. S. A. 110* (38), 15180−8.

(15) Eswar, N., Webb, B., Marti-Renom, M. A., Madhusudhan, M. S., Eramian, D., Shen, M. Y., Pieper, U., and Sali, A. (2006) Comparative protein structure modeling using Modeller. *Current protocols in bioinformatics*, Chapter 5, Unit 5.6, Wiley.

(16) Deng, D., Sun, P., Yan, C., Ke, M., Jiang, X., Xiong, L., Ren, W., Hirata, K., Yamamoto, M., Fan, S., and Yan, N. (2015) Molecular basis of ligand recognition and transport by glucose transporters. *Nature 526* (7573), 391−6.

(17) Malde, A. K., Zuo, L., Breeze, M., Stroet, M., Poger, D., Nair, P. C., Oostenbrink, C., and Mark, A. E. (2011) An Automated Force Field Topology Builder (ATB) and Repository: Version 1.0. *J. Chem. Theory Comput. 7* (12), 4026−4037.

(18) Morris, G. M., Huey, R., Lindstrom, W., Sanner, M. F., Belew, R. K., Goodsell, D. S., and Olson, A. J. (2009) AutoDock4 and AutoDockTools4: Automated docking with selective receptor flexibility. *J. Comput. Chem. 30* (16), 2785−91.

(19) Trott, O., and Olson, A. J. (2010) AutoDock Vina: improving the speed and accuracy of docking with a new scoring function, efficient optimization and multithreading. *J. Comput. Chem. 31* (2), 455−461.

(20) Hess, B., Kutzner, C., van der Spoel, D., and Lindahl, E. (2008) GROMACS 4: Algorithms for Highly Efficient, Load-Balanced, and Scalable Molecular Simulation. *J. Chem. Theory Comput. 4* (3), 435−47.

(21) Horta, B. A. C., Fuchs, P. F. J., van Gunsteren, W. F., and Hünenberger, P. H. (2011) New Interaction Parameters for Oxygen Compounds in the GROMOS Force Field: Improved Pure-Liquid and Solvation Properties for Alcohols, Ethers, Aldehydes, Ketones, Carboxylic Acids, and Esters. *J. Chem. Theory Comput. 7* (4), 1016−1031.

(22) Schmid, N., Eichenberger, A. P., Choutko, A., Riniker, S., Winger, M., Mark, A. E., and van Gunsteren, W. F. (2011) Definition and testing of the GROMOS force-field versions 54A7 and 54B7. *Eur. Biophys. J. 40* (7), 843−56.

(23) Hess, B., Bekker, H., Berendsen, H., and Fraaije, J. G. E. M. (1997) LINCS: A Linear Constraint Solver for Molecular Simulations. *J. Comput. Chem. 18*, 1463−1472.

DOI: 10.1021/acs.biochem.8b00607
Biochemistry 2018, 57, 6780−6786

(24) Miyamoto, S., and Kollman, P. A. (1992) Settle: An analytical version of the SHAKE and RATTLE algorithm for rigid water models. *J. Comput. Chem. 13*, 952−962.
(25) Smith, P. E., and van Gunsteren, W. (1994) Consistent dielectric properties of the simple point charge and extended simple point charge water models at 277 and 300 K. *J. Chem. Phys. 100*, 3169−3174.
(26) Hermans, J., Berendsen, H. J. C., Van Gunsteren, W. F., and Postma, J. P. M. (1984) A consistent empirical potential for water−protein interactions. *Biopolymers 23* (8), 1513−1518.
(27) Berendsen, H. J. C., Postma, J. P. M., van Gunsteren, W. F., DiNola, A., and Haak, J. R. (1984) Molecular dynamics with coupling to an external bath. *J. Chem. Phys. 81* (8), 3684−3690.
(28) Bussi, G., Donadio, D., and Parrinello, M. (2007) Canonical sampling through velocity rescaling. *J. Chem. Phys. 126* (1), 014101.
(29) Lemkul, J. A., and Bevan, D. R. (2010) Assessing the Stability of Alzheimer's Amyloid Protofibrils Using Molecular Dynamics. *J. Phys. Chem. B 114* (4), 1652−1660.
(30) Yang, R., Kolb, E. A., Qin, J., Chou, A., Sowers, R., Hoang, B., Healey, J. H., Huvos, A. G., Meyers, P. A., and Gorlick, R. (2007) The folate receptor alpha is frequently overexpressed in osteosarcoma samples and plays a role in the uptake of the physiologic substrate 5-methyltetrahydrofolate. *Clin. Cancer Res. 13* (9), 2557−67.
(31) Renukuntla, J., Shah, S., Boddu, S. H. S., Vadlapudi, A., Vadlapatla, R., Pal, D., and Mitra, A. (2015) Functional characterization and expression of folate receptor-β in T47D human breast cancer cells. *Drug Dev. Ther. 6* (2), 52−61.
(32) Li, K., Liu, Y., Zhang, S., Xu, Y., Jiang, J., Yin, F., Hu, Y., Han, B., Ge, S., Zhang, L., and Wang, Y. (2017) Folate receptor-targeted ultrasonic PFOB nanoparticles: Synthesis, characterization and application in tumor-targeted imaging. *Int. J. Mol. Med. 39* (6), 1505−1515.
(33) Hou, Z., Orr, S., and Matherly, L. H. (2014) Post-transcriptional regulation of the human reduced folate carrier as a novel adaptive mechanism in response to folate excess or deficiency. *Biosci. Rep. 34* (4), 457−468.
(34) Morales, C., Ribas, M., Aiza, G., and Peinado, M. (2005) Genetic determinants of methotrexate responsiveness and resistance in colon cancer cells. *Oncogene 24*, 6842−6847.
(35) Wu, J., Liu, Q., and Lee, R. J. (2006) A folate receptor-targeted liposomal formulation for paclitaxel. *Int. J. Pharm. 316* (1−2), 148−153.
(36) Ifergan, I., Jansen, G., and Assaraf, Y. G. (2008) The Reduced Folate Carrier (RFC) Is Cytotoxic to Cells under Conditions of Severe Folate Deprivation: RFC AS A DOUBLE EDGED SWORD IN FOLATE HOMEOSTASIS. *J. Biol. Chem. 283* (30), 20687−20695.

DOI: 10.1021/acs.biochem.8b00607
Biochemistry 2018, 57, 6780−6786